Proc. Natl. Acad. Sci. USA
Vol. 91, pp. 1721–1725, March 1994
Biochemistry

Structure of the *Escherichia coli* Fis–DNA complex probed by protein conjugated with 1,10-phenanthroline copper(I) complex

(protein–DNA interactions/chemical nuclease/DNA bending)

CLARK Q. PAN*, JIN-AN FENG*, STEVEN E. FINKEL†, RALF LANDGRAF†, DAVID SIGMAN*†‡, AND REID C. JOHNSON*†§

*Molecular Biology Institute, †Department of Biological Chemistry, School of Medicine, and ‡Department of Chemistry and Biochemistry, University of California, Los Angeles, CA 90024-1737

Communicated by Richard E. Dickerson, October 20, 1993 (received for review July 23, 1993)

ABSTRACT **The *Escherichia coli* Fis (*f*actor for *i*nversion *s*timulation) protein functions in many diverse biological systems including recombination, transcription, and DNA replication. Although Fis is a site-specific DNA-binding protein, it lacks a well-defined consensus recognition sequence. The electrophoretic mobility of Fis–DNA complexes, along with considerations of the Fis crystal structure, indicates that significant deformation of DNA occurs upon Fis binding. To investigate the structure of Fis–DNA complexes, the chemical nuclease 1,10-phenanthroline–copper complex (OP–Cu) has been linked to four specific sites within the Fis DNA-binding domain. Two of these Fis-OP derivatives were active in cleaving DNA. The scission patterns obtained on four different Fis binding sites indicate that Fis positions itself on these highly divergent DNA sequences in a very similar fashion. The patterns of cleavage of a derivative at Asn-98 generally support a model of a Fis–DNA complex that contains specific bends within the core-recognition sequence. Data from a second Fis-OP derivative at Asn-73 provides evidence for greater wrapping of flanking DNA around the sides of the Fis protein than was previously postulated. The cleavage efficiency of flanking segments varies, suggesting that the extent of DNA wrapping is sequence dependent. Specific amino acids on Fis are implicated in promoting this DNA wrapping.**

The *f*actor for *i*nversion *s*timulation (Fis) is a small basic protein in *Escherichia coli* that was initially identified because of its role in stimulating site-specific DNA inversion by the Hin and Gin recombinases. In this role, Fis binds site-specifically to a recombinational enhancer that becomes associated with the two recombination sites in a complex nucleoprotein structure. Fis has also been shown to function in phage λ site-specific recombination, transcriptional activation of rRNA and tRNA operons, repression of its own synthesis, and *oriC*-directed DNA replication (1). The x-ray crystal structure of Fis (2, 3) reveals it to be a homodimer with each 98-amino acid monomer containing four α-helices (Fig. 1). The helix–turn–helix DNA-binding domain of Fis is made up of the C-terminal C and D helices.

A comparison of over 35 Fis binding sites from various loci that have been analyzed by DNA cleavage inhibition studies (footprints) yields a degenerate 15-bp core sequence (1, 4). Gel electrophoresis of Fis–DNA complexes indicates that Fis induces significant DNA bending upon binding; bend angles of 40°–90° have been measured for different complexes. This bending of the DNA has been implicated as being important in Fis-mediated stimulation of phage λ excision and transcription (5–7). Considerable distortion of DNA is probably essential for Fis–DNA binding because the recognition α-helices (D and D′) are positioned only 25 Å from each other, which is too short a distance to insert into adjacent major grooves of straight B-DNA. In the absence of a Fis–DNA cocrystal structure, nuclease and chemical footprinting combined with mutation data were used to construct a model of Fis bound to the distal site of the Hin gene (*hin*) enhancer that contains a DNA bending angle of ≈60° (3, 8).

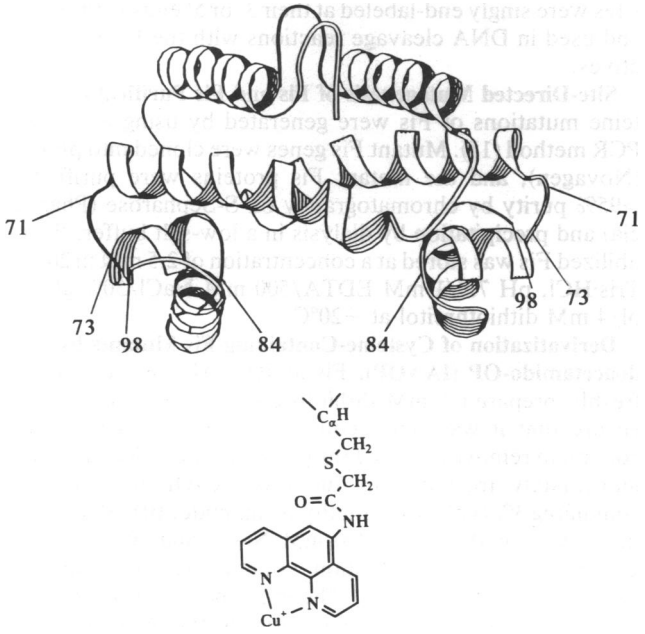

FIG. 1. (*Upper*) Ribbon diagram of Fis dimer, highlighting the positions of the four amino acids modified with 1,10-phenanthroline (OP) to probe Fis–DNA interactions. The N-terminal A α-helices are above the C-terminal C and D α-helices in this projection. (*Lower*) Structure of the OP-derivatized amino acid is shown below the Fis molecule.

To evaluate the accuracy of the model and to determine the structural similarities between Fis complexes at different DNA recognition sites, we have prepared a series of site-directed OP conjugates of Fis by a protocol of site-directed mutagenesis and chemical modification. These derivatives, which are capable of cleaving DNA in the presence of Cu^{2+} and thiol under aerobic conditions (9), allow us to identify with high resolution those nucleotides within Fis–DNA complexes that are positioned close to specific amino acids. The DNA scission patterns, along with the DNA binding properties of the mutants, support the overall model of a Fis–DNA complex but also reveal new aspects of Fis–DNA interac-

The publication costs of this article were defrayed in part by page charge payment. This article must therefore be hereby marked "*advertisement*" in accordance with 18 U.S.C. §1734 solely to indicate this fact.

Abbreviations: OP, 1,10-phenanthroline; IAAOP, 5′-iodoacetamido-OP; Fis, factor for inversion stimulation.

§To whom reprint requests should be sent at † address.

tions. In particular, evidence is obtained for additional wrapping of DNA flanking the 15-bp core region around the Fis dimer. Similar strategies have been used to probe the nature of other protein–DNA complexes (e.g., refs. 10–12).

MATERIALS AND METHODS

Fis Binding Sites. The *hin* distal and proximal enhancer sites are contained in pMS577 (13). The phage λ *attR* F site is located in pJT175 obtained from A. Landy (Brown University). The site I Fis binding site from the *rrnB* promoter is in pSL9 (7). The symmetrical 7-mer flank analog of the *hin* distal site was synthesized as two complementary 27-base oligonucleotides and cloned into the *Sma* I site of pUC18 to give pRJ1111. The DNA fragments containing the Fis binding sites were singly end-labeled at their 3′ or 5′ ends with ^{32}P (14) and used in DNA cleavage reactions with the Fis-OP derivatives.

Site-Directed Mutagenesis of Fis and Fis Purification. Cysteine mutations of Fis were generated by using a two-step PCR method (15). Mutant Fis genes were cloned into pET11a (Novagen), and the mutant Fis proteins were purified to >95% purity by chromatography on S-Sepharose (Pharmacia) and precipitation by dialysis in a low-salt buffer. Resolubilized Fis was stored at a concentration of 2.5 mM in 20 mM Tris·HCl, pH 7.5/1 mM EDTA/500 mM NaCl/50% glycerol/4 mM dithiothreitol at −20°C.

Derivatization of Cysteine-Containing Fis Mutants by 5-Iodoacetamido-OP (IAAOP). Fis at 100 μM was subjected to freshly prepared 1 mM dithiothreitol for 15 min at 4°C to ensure that it was fully reduced and then to a G-25 spin column to remove excess dithiothreitol. The reduced Fis was immediately treated with 700 μM IAAOP in a solution containing 3% (vol/vol) dimethylformamide, 10 mM Tris·HCl (pH 7.5), 1 mM EDTA, 200 mM NaCl, and 10% (vol/vol) glycerol in a 200-μl reaction volume. The reaction was incubated overnight at 4°C. The efficiency of alkylation was quantitated for the derivative carrying the Asn-73 → Cys change, called N73C, by assaying accessible thiol residues with Ellman's reagent, 5,5′-dithiobis(2-nitrobenzoic acid) (DTNB) (16). The DTNB assay indicated the presence of 1 mol of accessible thiol residue per mol of OP-underivatized Fis cysteine mutant subunit but only 0.05 mol of accessible thiol residue per mol of OP-derivatized Fis to give a 95% derivatization efficiency.

Gel Mobility-Shift Assay. A ^{32}P-labeled DNA fragment (10 pM) was mixed with various amounts of OP-derivatized or -underivatized Fis cysteine mutants in a solution containing 20 mM Tris·HCl (pH 7.5), 80 mM NaCl, 1 mM EDTA, and 100 μg of sonicated salmon sperm DNA per ml for 10 min at room temperature. The reaction mixture was then electrophoresed in an 8% polyacrylamide gel and analyzed by exposure to Kodak XAR x-ray film.

DNA Cleavage Reaction. The complex band obtained with each Fis-OP derivative in a gel mobility-shift assay was excised, crushed, and immersed in an equal volume of 100 μM $CuSO_4$/6 mM mercaptopropionic acid/6 mM H_2O_2/160 mM NaCl/40 mM Tris·HCl, pH 7.5/20 mM $MgCl_2$ for 2 hr at room temperature to induce DNA scission. The DNA scission reaction was quenched by adding 1/10th volume of 28 mM 2,9-dimethyl-1,10-phenanthroline, and the products were analyzed as described (17). DNA scission efficiency was estimated by scanning the autoradiogram with a LKB Ultroscan XL laser densitometer.

Modeling of Fis-OP Derivatives. Acetamido-OP was modeled onto the Fis–DNA complex by using the Insight II program (Biosym Technologies, San Diego).

RESULTS

Derivatization of Fis at Selected Sites with IAAOP. We have made four site-directed mutants of Fis that carry the Arg-71 → Cys, Asn-73 → Cys, Asn-84 → Cys, or Asn-98 → Cys mutations and are called R71C, N73C, N84C, and N98C; each was derivatized with IAAOP. The asparagine side chains at positions 73, 84, and 98 in the wild-type protein are predicted to make a contact with the phosphate backbone when bound to DNA according to the model of Yuan and coworkers (3, 8). The Asn-84 side chain is directed toward the center of the binding site and the Asn-73 and Asn-98 side chains are predicted to be contacting phosphates on the edges, with Asn-73 making the most distal contacts. The Arg-71 side chain is pointed toward the flanking DNA, though it does not directly contact DNA in our original model (3, 8). Substitution of these side chains with an OP on an acetamido segment linked to a cysteine (Fig. 1) has the potential to approach a C-1 H atom of a deoxyribose from the minor groove, the target of attack by the free OP–Cu complex (18).

Fis Mutant N98C-OP Derivative. N98C binds the *hin* enhancer distal site with the same affinity as wild-type Fis ($K_d \approx 1 \times 10^{-9}$ M) and with no apparent change in the mobility of the Fis-bound complex (Fig. 2). Derivatization of N98C with IAAOP has no effect on its binding characteristics. The N98C-OP–DNA complex band was excised from the gel along with the free DNA band as a control and incubated under conditions that induce scission by the OP–Cu^+ complex. As a further control, N98C was incubated with DNA in the presence of free OP, electrophoresed in parallel, and the complex band was excised and treated identically for DNA scission. No DNA cleavage was observed in the two controls (Fig. 3*A*, lanes 1 and 4; also data not shown). However, N98C-OP cleaves two regions on both the upper and lower strands of the *hin* enhancer distal site (Fig. 3*A*, lanes 2 and 5). The cleavage sites are symmetrically displaced with respect to the center of the binding site, and the lower strand cleavages are shifted several bases to the 3′ side of the upper-strand cleavage sites. This 3′ stagger is indicative of the approach of the OP–Cu^+ complex via the minor groove. Cleavage patterns by N98C-OP bound to three other sites, including the *hin* enhancer proximal site, the λ *attR* site, which functions in phage λ excision, and the site I of the *rrnB* P_1 promoter, which functions in transcriptional activation, were also analyzed. As summarized in Fig. 4, the sites and efficiencies of cutting are remarkably similar considering the difference in the recognition sequences. The overall single-strand cutting efficiency by N98C-OP at these sites was ≈1% on each side of the binding site.

Fis N73C-OP. Replacement of the asparagine with cysteine at position 73 reduced the apparent binding constant by a factor of ≈50. However, derivatization with IAAOP increases the affinity of the mutant protein for DNA by about a factor of 10. DNase I and *in situ* OP footprints of Fis–DNA

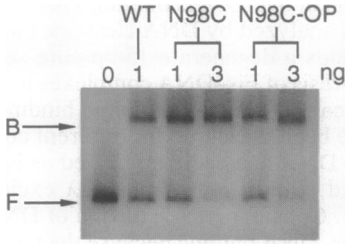

FIG. 2. Gel mobility-shift assay of wild-type (WT) Fis, mutant N98C, and derivatized N98C-OP binding to the *hin* distal enhancer site. The amount of protein used is indicated above each lane. Arrows point to the Fis-bound (B) and free (F) DNA bands.

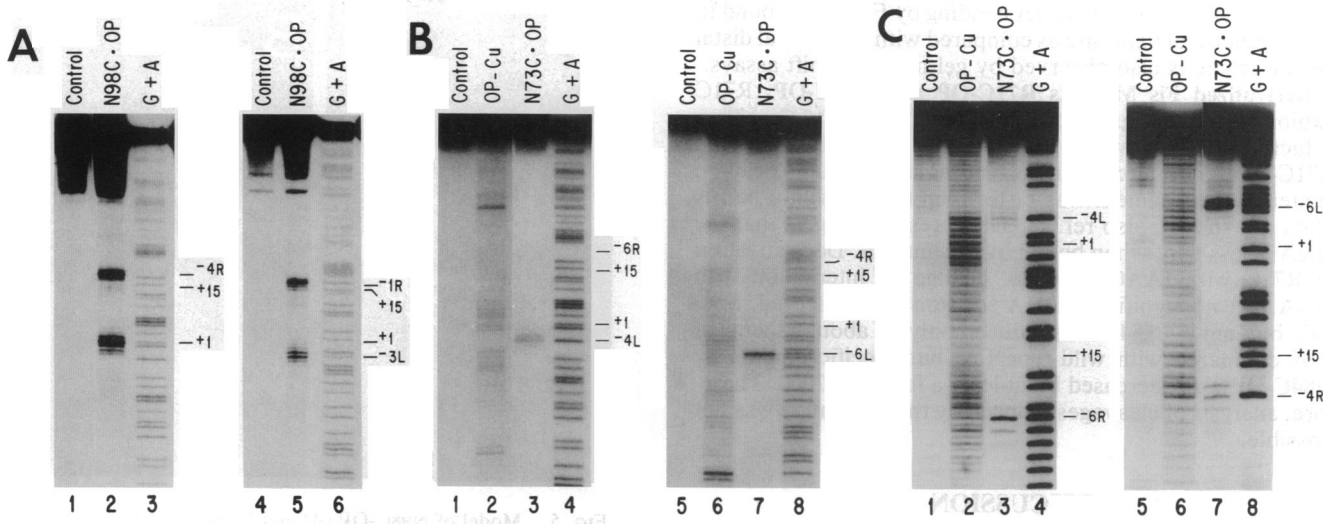

FIG. 3. DNA scission patterns by Fis-OP derivatives. (*A*) N98C-OP cleavage of the *hin* distal site. Lanes: 1–3 top strand; 4–6, bottom strand, both as depicted in Fig. 4. Free DNA band (lanes 1 and 4) and N98C-OP–DNA complex band (lanes 2 and 5) from the gel mobility-shift assay were isolated and subjected to DNA scission. (*B*) N73C-OP cleavage of the *hin* distal site. Lanes: 1–4 top strand; 5–8 bottom strand. Free DNA band (lanes 1 and 5) and N73C-OP–DNA complex band (lanes 3 and 7) were incubated under DNA-cleavage conditions. Free DNA probes were also subjected to DNA scission by free OP–Cu^+ (lanes 2 and 6). (*C*) N73C-OP cleavage of the "symmetrical" flank analog of the *hin* distal site. The lanes are identical to those in *B*. The 15-bp core sequence is numbered from +1 to +15; the left flank, from −10L to −1L; and the right flank, from −1R to −10R.

FIG. 4. Summary of the DNA scission patterns on five Fis binding sites by N98C-OP (open arrow) and N73C-OP (filled arrow). The DNA sequence of the 15-bp core region (uppercase letters, +1 to +15) along with 10 bp of each flank (lowercase letters, −1 to −10) are aligned for the five sites according to the core. The major cleavage sites are shown with the relative DNA scission efficiencies roughly proportional to the length of each arrow.

complexes showed a similar pattern of protections and enhancements for wild-type Fis, mutant N73C, and derivatized N73C-OP Fis. The migration of the DNA complexes with both the OP-derivatized and mutant N73C is somewhat faster than that of the wild-type complex when the binding site is located in the middle of a fragment, suggesting that the DNA may not be wrapped around these proteins to the same extent as with wild-type Fis. Nevertheless, the ability of N73C-OP to form specific complexes with DNA allows us to identify the nucleotides that are positioned close to the OP within the complex.

Fig. 3*B* shows the cleavages induced by N73C-OP within the upper (lane 3) and lower (lane 7) strands of the *hin* enhancer distal site. Reactivity within the left flanking region, as illustrated in Fig. 4, is more efficient than with N98C-OP, with 5–10% of the lower strand and 2–4% of the upper strand cleaved. Within the right flanking region, no cleavage was observed on the lower strand, and the yield was only ≈0.1% on the upper strand. Analysis of the cleavage patterns produced by N73C-OP at the other three Fis binding sites studied show cleavage efficiencies that are more equivalent between their respective flanking sequences (summarized in Fig. 4). The locations of the cleavage sites when present within the different binding sites are all similar, extending up to 4 bp on the 5′ side and 7 bp on the 3′ side of the core-binding sequence.

The dramatic difference in cleavage efficiency of the flanking sequences of the *hin* enhancer distal site by N73C-OP suggests that the DNA may be wrapped around Fis to a different extent on the left side of the site as compared with the right side. To explore the importance of the flanking sequences in influencing this process, we constructed a variant of the *hin* enhancer distal site in which the 7-bp left flanking sequence was duplicated on both sides (see "sym. flank" in Fig. 4). The efficiency of cleavage by N73C-OP on both sides of this site was much more equivalent, with a ratio of left to right side cutting of ≈2:1 (Fig. 3*C*, lanes 3 and 7) as compared with ≈70:1 with the wild-type sequence (Fig. 3*B*, lanes 3 and 7). However, the extent of cleavage on the left side of the synthetic Fis site was less than that observed with the wild-type sequence, suggesting that sequences beyond the 7-bp region in the flank may also contribute to DNA

bending. Greater overall DNA bending by Fis when bound to the symmetrical flank site as compared with the normal distal enhancer site is also observed by gel-mobility shift assays.

Derivatized Fis Mutants R71C-OP and N84C-OP. R71C exhibited only a slight decrease in binding affinity (less than a factor of 2). However, like N73C, the mobility of the R71C–DNA complex when the binding site is located near the center of the fragment was faster than that of wild-type Fis (data not shown; also ref. 7). These results suggest that the DNA is less bent when bound by this mutant. Derivatization of R71C with IAAOP did not change its interaction with DNA, yet no significant DNA scission was observed. Specific binding by N84C was reduced only by about a factor of 2 as compared with wild-type Fis, but specific binding by N84C-OP was decreased by at least a factor of 1000. Therefore, analysis of cleavages induced by this derivative was not possible.

DISCUSSION

We have constructed four Fis-OP derivatives in order to investigate the molecular interaction between Fis and DNA. The selection of residues on Fis for addition of the DNA cleavage moiety was guided by our working model of a Fis–DNA complex (3, 8). These sites were predicted to allow the close approach of the OP moiety to the C-1 H of one or more deoxyriboses. The C-1 H of the deoxyribose is most likely the principal site of oxidative attack by the Fis-OP chimeras because it is the reactive position in DNA cleavage by the free 2:1 complex of OP-Cu^+ (18). An alternative site of attack is the C-4 H, but oxidation at that position would generate 3′-phosphoglycolates, not 3′-phosphomonoesters, and there is no evidence for the formation of this product by gel electrophoresis (Fig. 3).

The DNA scission pattern of two of the Fis-OP derivatives on four different DNA binding sites allows us to confirm certain aspects of the working model and infer several new features. One of the most important conclusions is that the overall mode of Fis interaction with target sites containing highly divergent DNA sequences is very similar. The relative locations of the DNA cleavages induced by each Fis-OP derivative at the four binding sites are virtually identical. These four sites, which are found in different biological contexts, have only 3 of the 15 core nucleotides in common with each other if one considers both orientations.

While the location of the Fis dimer relative to the 15-bp core sequence is similar in the different Fis–DNA complexes, analysis of the cleavage efficiencies by N73C-OP within the flanking DNAs suggests significant structural variations. Of the eight half-sites investigated, the left half of the *hin* enhancer distal site yields by far the strongest cleavage by this derivative. The right half of this same site is the least efficiently cleaved. This implies that the flanking sequence on the left side of the *hin* enhancer distal site tends to be in close contact with Fis, while the flanking sequence on the right side is not.

The importance of the particular nucleotide sequence within the flanking regions in determining the extent of DNA wrapping around Fis has been demonstrated by the synthesis of a modified enhancer distal recognition sequence that contains 7 bp of left flanking sequence (5′-cttacta-3′ in Fig. 4) repeated on the right side in inverted orientation. The presence of these 7 bp results in substantially more efficient cleavage within the right flanking sequence, although the efficiency is not as high as with the left side. Possibly, these 7 bp are not the only determinants of DNA bending. The difference in the chemical reactivity is not attributable to the nucleotide structure because the nuclease activity is directed to the deoxyribose moiety and should not be influenced by the base linked to the attacked deoxyribose. Indeed, the left flanking region, which is cleaved with high efficiency with N73C-OP, does not display hypersensitivity to the OP–Cu complex or 5-phenyl-OP in the presence or absence of wild-type Fis (Fig. 3*B*, lanes 2 and 6; also data not shown).

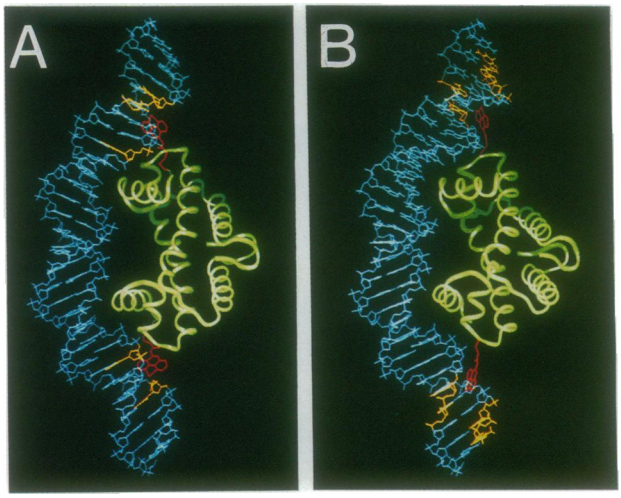

FIG. 5. Model of N98C-OP (*A*) and N73C-OP (*B*) binding to the *hin* enhancer distal site based on our working model of a Fis–DNA complex. The DNA (blue) is oriented so that the left flanking sequence is on the top with the nucleotides cleaved by the Fis-OP derivatives highlighted in yellow. The highlighted nucleotides for N73C-OP reflect the positions cleaved in the binding site containing the symmetrical flanking sequence, since almost no cutting on the right side of the *hin* enhancer distal site is observed. The Fis protein is in green, with the OP linked to amino acids 73 or 98 depicted in red. Note that while the OP attached to residue 98 in *A* can be positioned within ≈4 Å of each of the cleaved nucleotides in the model, the OP attached to residue 73 cannot reach the cleaved nucleotides, indicating further DNA bending is required.

Model of the Fis–DNA Complex. The cleavage results support the postulated model with respect to the positioning of the protein relative to the 15-bp core sequence. For example, the model indicates that aa 73 is more distant from the dyad axis than aa 98. This is reflected precisely in the DNA scission patterns, since the sites cleaved by N73C-OP are located 1–3 bases beyond those cleaved by N98C-OP. The DNA cleavage patterns of N98C-OP are entirely consistent with the proposed location of the Asn-98 side chain relative to the DNA (Fig. 5*A*). The copper coordinated to Fis-linked OP can be fit within 4 Å of the C-1 H atom of all of the cleaved deoxyriboses (highlighted in yellow) by slightly rotating the single bonds of the OP linker segment. The radical generated upon Cu^+ oxidation should be coordinated and will attack the closest C-1 H of deoxyribose. The distance between the copper ion and the C-1 H is predicted to be the sum of the bond lengths of copper to radical (possibly an oxygen atom) and radical to C-1 H. This distance is estimated to be 3 Å, slightly less than the 4 Å measured in the model (Fig. 5*A*). This may explain why the DNA scission efficiency of N98C-OP is relatively low.

The cleavage pattern with N98C-OP provides direct evidence for significant bending within the core-recognition sequence. The most extended distance that enables DNA to contact OP-coordinated Cu when linked to residue 98 of each subunit is 57 Å. However, N98C-OP typically cleaves at 2 bp that are 19 bases or 64.5 Å apart if one assumes standard B-DNA parameters. The only way to reconcile these divergent distances is if the DNA is bent in the Fis–DNA complex. Based on these considerations, a DNA bending angle between the sites cleaved by N98C-OP is calculated to be ≈50°.

According to the Fis–DNA model, Asn-73 contacts the phosphate backbone via hydrogen bonding. Loss of this hydrogen bond in the N73C mutant results in a significant

decrease in DNA binding affinity, in contrast to N98C, suggesting that Asn-73 plays a more important role than Asn-98 in stabilizing the Fis–DNA complex. The decrease with N73C cannot be attributed to the deprotonation of the sulfhydryl group of cysteine, since the mutant has the same DNA binding affinity at pH 7.5 or at pH 6 (data not shown). The lowered DNA affinity in the mutant is partially restored upon OP-derivatization possibly because of the presence of the amide in the linker between N73C and OP functioning as a hydrogen bond donor to the phosphate backbone of DNA. This was further supported by derivatizing N73C with iodoacetate or iodoacetamide. The iodoacetate derivative displayed drastically reduced binding, presumably because of the negative charge of the carboxylate, while the iodoacetamide derivative increases binding, consistent with the hydrogen bonding capability of the amide.

The cleavage results with N73C-OP indicate that the DNA within the flanking regions would have to be bent more than the model has suggested. In the present model, in which we have not introduced any curvature into the DNA beyond the core nucleotides, the OP cannot be positioned sufficiently close to the cleaved nucleotides; the closest approach of the OP to the C-1 H of the cleavage sites ranges from 5 to 10 Å (Fig. 5*B*). Analogous to the calculation done for N98C-OP, we estimate an overall Fis-induced bending angle of ≈70° for the 25-bp region that includes the 15-bp core and 5 bp of each flank. The cleavage results by N73C-OP may reflect a minimum estimate of bending in a wild-type complex, since gel mobility-shift assays suggest that substitutions at Asn-73 can lead to a reduction in bending.

Modification of R71C with IAAOP failed to give a derivative capable of cleaving the *hin* enhancer distal sequence even though the modified protein binds to the target sequence with high affinity. We believe that this arginine provides a critical contact that promotes additional bending of the flanking sequences. Thus, loss of this side chain leads to less overall bending, as revealed by the gel mobility of the complexes, and results in the failure of R71C-OP to cleave DNA.

Conversion of residue 84 to a cysteine followed by its modification with IAAOP generates a derivative that completely loses its specific DNA affinity. This position was chosen for OP attachment because it was close to the C-2 axis of the protein. By analogy to prior studies with the *E. coli trp* repressor (17), this would be expected to yield a chimeric protein capable of efficient double-stranded cleavage activity. However, the addition of OP at this central location must sterically block the close approach of Fis to its DNA recognition sequence.

Perspective. These experiments also provide insight into the geometry of the copper–oxo species directly responsible for the observed oxidative attack. At issue is the precise location of the metal-bound oxene or hydroxyl radical. In the case of the untargeted tetrahedral Cu^+ complex, it is likely that hydrogen peroxide coordinates directly to the Cu^+ and forms a tetragonal pyramid prior to releasing hydroxide ion from the $(OP)_2Cu^+$–H_2O_2 complex. In the case where the OP is tethered to a carrier ligand such as the Fis protein, only a single OP is necessary for cleavage. The geometry, and indeed the ligands that complete the coordination sphere of the Cu^+, are difficult to infer. Whether they are water or Tris molecules in a tetragonal pyramid, molecular modeling of N98C-OP suggests that the most likely coordination site of the oxidative species is the axial position. Therefore, the molecular modeling of the Fis-OP chimeras provides interesting and unusual insight into the chemical mechanism of the nuclease activity of the OP-Cu^+ complex.

The Fis N73C-OP derivative should be a useful tool for identifying sequences that contribute to DNA bendability. This aspect of the Fis–DNA interaction is distinguishable from the affinity of a particular sequence for Fis and may be relevant to its biological activity in particular reactions. If the double-stranded cutting efficiency of N98C-OP or N73C-OP can be improved, these chimeras may be useful in identifying as yet unknown sites of interaction of Fis within the *E. coli* chromosome. One possible way to improve scission may be to use a longer linker arm in attaching OP. This approach has been successfully used in studies by Ebright and colleagues (19) to increase the cutting efficiency of OP derivatives of the catabolite activator protein. An efficient DNA scission reagent derived from Fis would also be a novel "restriction enzyme," with potential application in chromosome mapping, cloning, and sequencing.

We thank Dr. Chi-hong B. Chen, Dr. Abhijit Mazumder, Joyce Soong, Chris Sutton, Dr. Robert Osuna, and David Perrin for important discussions. This work was made possible by National Institutes of Health Grants GM-21199 to D.S. and GM-38509 to R.C.J. C.P. was supported by U.S. Department of Health and Human Services Biotechnology Training Program GNO8375, R.L. was supported by a Merck predoctoral fellowship, and S.E.F. was supported in part by National Research Service Award GM-07104 and a Dr. Ursula Mandel Fellowship.

1. Finkel, S. & Johnson, R. (1992) *Mol. Microbiol.* **6,** 3257–3266.
2. Kostrewa, D., Granzin, J., Koch, C., Choe, H.-W., Raghunathan, S., Wolf, W., Labahn, J., Kahmann, R. & Saenger, W. (1991) *Nature (London)* **349,** 178–180.
3. Yuan, H., Finkel, S., Feng, J.-A., Kaczor-Grzeskowiak, M., Johnson, R. & Dickerson, R. (1991) *Proc. Natl. Acad. Sci. USA* **88,** 9558–9562.
4. Hübner, P. & Arber, W. (1989) *EMBO J.* **8,** 577–585.
5. Thompson, J. F., Moitoso de Vargas, L., Koch, C., Kahmann, R. & Landy, A. (1987) *Cell* **50,** 901–908.
6. Osuna, R., Finkel, S. & Johnson, R. (1991) *EMBO J.* **10,** 1593–1603.
7. Gosink, K., Ross, W., Leirmo, S., Osuna, R., Finkel, S., Johnson, R. & Gourse, R. (1993) *J. Bacteriol.* **175,** 1580–1589.
8. Feng, J.-A., Yuan, H., Finkel, S., Johnson, R., Kaczor-Grzeskowiak, M. & Dickerson, R. (1992) in *Structure and Function*, eds. Sarma, R. H. & Sarma, M. H. (Adenine, Schenectady, NY), Vol. 2, pp. 1–9.
9. Sigman, D. & Chen, C.-H. (1990) *Annu. Rev. Biochem.* **59,** 207–236.
10. Chen, C.-H. B. & Sigman, D. S. (1987) *Science* **237,** 1197–1201.
11. Sluka, J. P., Horvath, A. C., Glasgow, A. C., Simon, M. I. & Dervan, P. B. (1987) *Science* **238,** 1129–1132.
12. Ebright, R. H., Ebright, Y. W., Pendergrast, P. S. & Gunasekera, A. (1990) *Proc. Natl. Acad. Sci. USA* **87,** 2882–2886.
13. Johnson, R. & Simon, M. (1985) *Cell* **41,** 781–791.
14. Sambrook, J., Fritsch, E. & Maniatis, T. (1989) *Molecular Cloning: A Laboratory Manual* (Cold Spring Harbor Lab. Press, Plainview, NY).
15. Landt, O., Grunert, H. & Hahn, U. (1990) *Gene* **96,** 125–128.
16. Riddles, P., Blakeley, T. & Zerner, B. (1983) *Methods Enzymol.* **91,** 49–60.
17. Sutton, C., Mazumder, A., Chen, C.-H. & Sigman, D. (1993) *Biochemistry* **32,** 4225–4230.
18. Goyne, T. E. & Sigman, D. S. (1987) *J. Am. Chem. Soc.* **109,** 2846–2848.
19. Pendergrast, P. S., Ebright, Y. W. & Ebright, R. H. (1993) *J. Cell. Biochem.* **17,** 156 (abstr.).